sciendo

CAIM
ISSN 2038-0909

Commun. Appl. Ind. Math. 12 (1), 2021, 1–12 DOI: 10.2478/caim-2021-0001

Research Article

Numerical methods for a system of coupled Cahn-Hilliard equations

Mattia Martini[1] , Giacomo E. Sodini[1*]

[1]Dipartimento di Matematica, Politecnico di Milano, Milano 20133, Italy

[*]Email address for correspondence: giacomoenrico.sodini@mail.polimi.it

Communicated by Roberto Natalini

Received on 10 08, 2020. Accepted on 03 16, 2021.

Abstract

In this work, we consider a system of coupled Cahn-Hilliard equations describing the phase separation of a copolymer and a homopolymer blend. We propose some numerical methods to approximate the solution of the system which are based on suitable combinations of existing schemes for the single Cahn-Hilliard equation. As a verification for our experimental approach, we present some tests and a detailed description of the numerical solutions' behaviour obtained by varying the values of the system's characteristic parameters.

Keywords: `Coupled Cahn-Hilliard equation, Finite Element Method, phase separation model.`

AMS subject classification: `65Z05, 65M60.`

1. Introduction

The Cahn-Hilliard equation is a fourth order nonlinear PDE introduced in [1–3] to model the phase separation in binary systems. This equation and its variants present many practical applications, see for example [4–6]. In the last decades, many methods and numerical techniques to treat this kind of equations have been developed. See [7] and [8] for a review of the numerical and theoretical results respectively.

The system we study describes the spontaneous separation that occurs in a copolymer (made of two monomers) and a homopolymer (made of one monomer) blend. The diffuse interface model we consider avoids the explicit treatment of the sharp interface condition between the copolymer and the homopolymer and it has been accurately investigated in a three-dimensional setting in [9], using the numerical methods developed in [10] and [11].

In this work we study the two-dimensional case, using a different numerical technique, namely Finite Element Method (FEM). In particular, we adapt some basic techniques used for the single Cahn-Hilliard equation and suitably couple them in order to deal with the fully coupled system. Since we do not carry out a theoretical analysis of our techniques, we check that the results we obtain reflect the physical properties of the system; to do so we describe the behaviour of the numerical solutions for different values of the characteristic parameters of the system verifying in this way that the physical properties of the system are well represented in our simulations.

The paper is structured as follows: in Section 2 we introduce the mathematical model we consider; in Section 3 we present the numerical methods for the single equation that will constitute the building blocks for our algorithms; in Section 4 we describe the behaviour of the numerical solutions obtained by varying the parameters of the system; in Section 5, we draw some conclusions and we discuss some possible further developments.

2. The mathematical model

In this section we give a brief description of the model whose detailed derivation can be found in [12]. The system we consider consists of a copolymer and a homopolymer blend. Two phase separations occur: macrophase separation and microphase separation. The first one takes place between the copolymer and the homopolymer and it is represented by the order parameter u, which takes values in $[-1, 1]$. The ending

points of this interval correspond to a homopolymer rich domain (-1) and a copolymer rich domain ($+1$). The microphase separation is described by the order parameter v and takes place inside the copolymer, between its two component, say A and B. The function v also takes values in $[-1,1]$ with ending points corresponding to A and B rich domains, respectively.

We focus on the two-dimensional case, mainly due to computational reasons and we study the problem with homogeneous Neumann boundary conditions. Notice that this is a different situation from [9], where periodic boundary conditions are considered.

Let $\Omega \subset \mathbb{R}^2$ be a bounded Lipschitz domain, let $\epsilon_u, \epsilon_v, \tau_u, \tau_v, T, \sigma > 0$ and let $\alpha, \beta, \bar{v} \in \mathbb{R}$. The model we consider is given by the following system of coupled Cahn-Hilliard equations:

$$
(1) \qquad \begin{cases} \tau_u u_t = -\Delta\{\epsilon_u^2 \Delta u + (1-u)(1+u)u - \alpha v - \beta v^2\} & \text{in } \Omega \times [0,T], \\ \tau_v v_t = -\Delta\{\epsilon_v^2 \Delta v + (1-v)(1+v)v - \alpha u - 2\beta uv\} - \sigma(v-\bar{v}) & \text{in } \Omega \times [0,T], \\ u(\cdot,0) = u_0 & \text{in } \Omega, \\ v(\cdot,0) = v_0 & \text{in } \Omega, \\ \partial_{\mathbf{n}} u = \partial_{\mathbf{n}}\{\epsilon_u^2 \Delta u + (1-u)(1+u)u - \alpha v - \beta v^2\} = 0 & \text{on } \partial\Omega \times [0,T], \\ \partial_{\mathbf{n}} v = \partial_{\mathbf{n}}\{\epsilon_v^2 \Delta v + (1-v)(1+v)v - \alpha u - 2\beta uv\} = 0 & \text{on } \partial\Omega \times [0,T], \end{cases}
$$

where $\mathbf{n}$ is the outward normal of Ω and $u_0, v_0 : \Omega \to \mathbb{R}$ are given initial conditions.

Notice that the second equation is a Cahn-Hilliard-Ono equation due to the presence of $\sigma(v-\bar{v})$. The time constants τ_u, τ_v control the speed of the evolution of u and v and, specifically, to smaller coefficients correspond a faster evolution. The parameters ϵ_u, ϵ_v are proportional to the thickness of the propagation fronts of each component and they control the size of the interface between the macrophases and the microphases. The parameter σ is related to the bonding between A and B in the copolymer and it controls the nonlocal interactions in the second equation. More details on the nonlocal effects in phase separation problems can be found in [13]. From a practical point of view, values of σ different from zero prevent the copolymer from forming large macroscopic domains. As σ grows, finer structures and different morphologies arise. The first coupling parameter α controls the interaction between the confined copolymer and the confining surface. If $\alpha = 0$, the configuration is symmetric and thus u has the same preference for any value of v. If $\alpha \neq 0$, the configuration's symmetry is broken, meaning that u has preference for one specific block of the copolymer. The coupling parameter β affects the free energy depending of the value of u, as $v^2 > 0$. Finally, the average value of v in Ω is represented by $\bar{v}$ and T is the time horizon.

As a final remark we highlight that, as explained in [9], the state dynamics of these two coupled systems evolves as a gradient flow, up to the reaction term. More precisely, the state variables minimize the value of the following energy functional:

$$
(2) \qquad F \equiv F_{\epsilon_u,\epsilon_v,\sigma}(u,v) = \int_\Omega \left\{ \frac{\epsilon_u^2}{2}|\nabla u|^2 + \frac{\epsilon_v^2}{2}|\nabla v|^2 + W(u,v) + \frac{\sigma}{2}|(-\Delta)^{-1/2}(v-\bar{v})|^2 \right\},
$$

where

$$
(3) \qquad W(u,v) = \frac{(u^2-1)^2}{4} + \frac{(v^2-1)^2}{4} + \alpha uv + \beta uv^2.
$$

3. Numerical approximations

Before presenting our numerical strategies to approximate the solution of (1), we revise some known techniques for the single Cahn-Hilliard equation. Let us introuce the chemical potentials of the Cahn-Hilliard equations:

$$
(4) \qquad w_u := \epsilon_u^2 \Delta u + (1-u)(1+u)u - \alpha v - \beta v^2, \quad w_v := \epsilon_v^2 \Delta v + (1-v)(1+v)v - \alpha u - 2\beta uv
$$

and let us set $\phi(x) := (1-x^2)x$. Then (1) becomes

$$
\begin{cases}
\tau_u u_t = -\Delta w_u & \text{in } \Omega \times [0,T], \\
w_u = \epsilon_u^2 \Delta u + \phi(u) - \alpha v - \beta v^2 & \text{in } \Omega \times [0,T], \\
\tau_v v_t = -\Delta w_v - \sigma(v - \overline{v}) & \text{in } \Omega \times [0,T], \\
w_v = \epsilon_v^2 \Delta v + \phi(v) - \alpha u - 2\beta uv & \text{in } \Omega \times [0,T], \\
u(\cdot,0) = u_0 & \text{in } \Omega, \\
v(\cdot,0) = v_0 & \text{in } \Omega, \\
\partial_{\mathbf{n}} u = \partial_{\mathbf{n}} v = \partial_{\mathbf{n}} w_u = \partial_{\mathbf{n}} w_v = 0 & \text{on } \partial\Omega \times [0,T],
\end{cases} \tag{5}
$$

which is now a system of second order coupled PDEs.

3.1. *Semi-discretization in time*

In this section we introduce the semi-discretization in time. Let us fix $n > 0$, $\Delta t = T/n$ and consider a discretization of $[0,T]$ given by $\{0 = t_0, t_1, \dots, t_n = T\}$, where $t_k = k\Delta t$ and let us set $u(t_k) := u^{(k)}$ (analogously for v, w_u, w_v). Consider the following approximation for the time derivative of u

$$
u_t \approx \frac{u^{(k+1)} - u^{(k)}}{\Delta t}, \tag{6}
$$

and the same for v. By multiplying (5) by the test functions $\varphi, \eta, \psi, \zeta$ and integrating in space over Ω, we obtain: find $\{(u^{(k)}, v^{(k)}, w_u^{(k)}, w_v^{(k)})\}_{k=0,\dots,n} \subset [H^1(\Omega)]^4$ s.t.

$$
\begin{cases}
\displaystyle\int_\Omega \tau_u \frac{u^{(k+1)} - u^{(k)}}{\Delta t}\varphi = \int_\Omega \nabla w_u^{(k+1)} \cdot \nabla \varphi, \\
\displaystyle\int_\Omega w_u^{(k+1)}\eta = \int_\Omega \{-\epsilon_u^2 \nabla u^{(k+1)} \cdot \nabla \eta + \phi(u^{(k+1)})\eta - \alpha v^{(k+1)}\eta - \beta (v^{(k+1)})^2 \eta\}, \\
\displaystyle\int_\Omega \tau_v \frac{v^{(k+1)} - v^{(k)}}{\Delta t}\psi = \int_\Omega \{\nabla w_v^{(k+1)} \cdot \nabla \psi - \sigma(v^{(k+1)} - \overline{v})\psi\}, \\
\displaystyle\int_\Omega w_v^{(k+1)}\zeta = \int_\Omega \{-\epsilon_v^2 \nabla v^{(k+1)} \cdot \nabla \zeta + \phi(v^{(k+1)})\zeta - \alpha u^{(k+1)}\zeta - 2\beta u^{(k+1)} v^{(k+1)} \zeta\}, \\
u^{(0)} = u_0, \\
v^{(0)} = v_0,
\end{cases} \tag{7}
$$

for every $0 \le k \le n-1$ and for every $\varphi, \eta, \psi, \zeta \in H^1(\Omega)$.

3.2. *Full discretization*

To introduce the space discretization of (7) based on FEM, we project the semi-discretized problem on a finite dimensional Hilbert space $V_h \subset H^1(\Omega)$. Then the Galerkin approximation of (7), is: find

$\{(u_h^{(k)}, v_h^{(k)}, w_{u,h}^{(k)}, w_{v,h}^{(k)})\}_{k=0,\dots,n} \subset V_h^4$ s.t.

$$
(8)\qquad \begin{cases} \displaystyle\int_\Omega \tau_u \frac{u_h^{(k+1)} - u_h^{(k)}}{\Delta t}\varphi_h = \int_\Omega \nabla w_{u,h}^{(k+1)} \cdot \nabla \varphi_h, \\ \displaystyle\int_\Omega w_{u,h}^{(k+1)}\eta_h = \int_\Omega \{-\epsilon_u^2 \nabla u_h^{(k+1)} \cdot \nabla \eta_h + \phi(u_h^{(k+1)})\eta_h - \alpha v_h^{(k+1)}\eta_h - \beta (v_h^{(k+1)})^2 \eta_h\}, \\ \displaystyle\int_\Omega \tau_v \frac{v_h^{(k+1)} - v_h^{(k)}}{\Delta t}\psi_h = \int_\Omega \{\nabla w_{v,h}^{(k+1)} \cdot \nabla \psi_h - \sigma(v_h^{(k+1)} - \overline{v})\psi_h\}, \\ \displaystyle\int_\Omega w_{v,h}^{(k+1)}\zeta_h = \int_\Omega \{-\epsilon_v^2 \nabla v_h^{(k+1)} \cdot \nabla \zeta_h + \phi(v_h^{(k+1)})\zeta_h - \alpha u_h^{(k+1)}\zeta_h - 2\beta u_h^{(k+1)} v_h^{(k+1)}\zeta_h\}, \\ u_h^{(0)} = u_{0,h}, \\ v_h^{(0)} = v_{0,h}, \end{cases}
$$

for every $0 \le k \le n-1$ and for every $\varphi_h, \eta_h, \psi_h, \zeta_h \in V_h$, where $u_h^{(k)}, v_h^{(k)}, w_{u,h}^{(k)}, w_{v,h}^{(k)}, u_{0,h}, v_{0,h}$ are the projection of $u^{(k)}, v^{(k)}, w_u^{(k)}, w_v^{(k)}, u_0, v_0$ on V_h respectively.

In order to construct such a space, we consider a triangular conforming mesh $\mathcal{T}_h(\Omega)$, where $h = \max_{K\in\mathcal{T}_h} \operatorname{diam}(K)$. A family of possible choices for V_h is

$$
(9)\qquad P_r = \{v_h \in C^0(\bar{\Omega})\colon v_h|_K \in \mathbb{P}_r(K), \forall K \in \mathcal{T}_h(\Omega)\}, \quad r \in \mathbb{N},
$$

where $\mathbb{P}_r(K)$ is the space of r degree polynomials defined over K. For a more detailed theoretical framework see, for example, Chapter 4 in [14].

3.3. *Linearization*

In this section, we introduce suitable linear approximations for the nonlinear terms $\phi(u^{(k+1)})$ and $\phi(v^{(k+1)})$ and for the coupling terms $(v^{(k+1)})^2$ and $u^{(k+1)}v^{(k+1)}$.

For the last two terms we use the following approximations:

$$
(10)\qquad (v^{(k+1)})^2 \approx v^{(k)}v^{(k+1)}, \quad u^{(k+1)}v^{(k+1)} \approx u^{(k)}v^{(k+1)}.
$$

The first one is the simplest possible choice and seems to be natural. On the other hand, we expect u to evolve faster than v, see [9], and this motivates our choice for the second linearization. Indeed, since u will reach a stationary condition before v, we can reasonably suppose that after the initial macrophase separation, the error introduced by considering $u^{(k)}$ instead of $u^{(k+1)}$ will be smaller that the one introduced by considering $v^{(k)}$ instead of $v^{(k+1)}$.

The key point is now to find suitable approximations for the potentials $\phi(u^{(k+1)})$ and $\phi(v^{(k+1)})$. To this aim, we propose the following linearization strategies:

1. Optimal dissipation method (OD2) both for u and v, i.e.

$$
(11)\qquad \phi(u^{(k+1)}) = -\frac{3}{2}(u^{(k)})^2 u^{(k+1)} + \frac{1}{2}(u^{(k)})^3 + \frac{u^{(k+1)} + u^{(k)}}{2},
$$

see [15], were the authors develop the so-called optimal dissipation approach, which is based on a second order in time linear approximation of the potential term. In the single Cahn-Hilliard equation case, this approximation gives a second order in time linear scheme.

2. Wu-Van Zwieten-Van der Zee's method (WVV) both for u and v:

$$\phi(u^{(k+1)}) = \begin{cases} 2u^{(k+1)} + u^{(k+1)} - u^{(k)} - 2 & \text{if } u^{(k)} < -1, \\ 2u^{(k+1)} + u^{(k+1)} - u^{(k)} + 3u^{(k)} - (u^{(k)})^3 & \\ \quad + \dfrac{1}{2}(u^{(k+1)} - u^{(k)})(3 - 3(u^{(k)})^2) & \text{if } u^{(k)} \in [-1, 1], \\ 2u^{(k+1)} + u^{(k+1)} - u^{(k)} + 2 & \text{if } u^{(k)} > 1. \end{cases} \tag{12}$$

which is discussed in [16]. Here the authors consider a diffuse-interface tumor-growth system consisting of a reactive Cahn-Hilliard equation and a reaction-diffusion equation. The schemes are of the Crank-Nicolson type with a convex-concave splitting of the free-energy. The potential term is approximated employing an implicit Taylor expansion of the convex part and an explicit one of the non-convex part. The splitting considered for the potential term is

$$F(u) = \begin{cases} \left(u^2 + \dfrac{1}{4}\right) - \left(-2u - \dfrac{3}{4}\right) & \text{if } u < -1, \\ \left(u^2 + \dfrac{1}{4}\right) - \left(\dfrac{3}{2}u^2 - \dfrac{1}{4}u^4\right) & \text{if } u \in [-1, 1], \\ \left(u^2 + \dfrac{1}{4}\right) - \left(2u - \dfrac{3}{4}\right) & \text{if } u > 1. \end{cases} \tag{13}$$

Moreover, this method stabilizes the system by modifying the second and the fourth equations of (7) as follows:

$$\begin{aligned} \int_\Omega w_u^{(k+1)}\psi = &\int_\Omega \{-\frac{\epsilon^2}{2}\nabla u^{(k+1)} \cdot \nabla\psi + \phi(u^{(k+1)})\psi\} \\ &+ \left[\int_\Omega \{-\frac{\epsilon^2}{2}\nabla u^{(k)} \cdot \nabla\psi - \alpha\nabla(u^{(k+1)} - u^{(k)}) \cdot \nabla\psi\}\right], \end{aligned} \tag{14}$$

where $\alpha > 0$ is a stabilization parameter. The expression in squared brackets is completely new and in addition there is a weighted contribution of $\nabla u^{(k+1)}$ which is multiplied by $\frac{1}{2}$. Clearly the same applies to v. According to [15], this method is second order accurate both in space and time in the single Cahn-Hilliard equation case.

3. Eyre's method (EY), both for u and v:

$$\phi(u^{(k+1)}) = -2u^{(k+1)} - (u^{(k)})^3 + 3u^{(k)}. \tag{15}$$

The key point in Eyre's work [17] is to approximate the potential term by introducing a positive phobic numerical dissipation in the discrete energy law, to ensure the unconditional energy-stability of the scheme.

4. Linear splitting method (LS) both for u and v; i.e.

$$\phi(u^{(k+1)}) = (1 - u^{(k)})(1 + u^{(k)})u^{(k+1)}, \tag{16}$$

suggested in [9].To treat nonlinearities, the cubic term is split into the product of two terms; the first one is quadratic and related to the state of the system at the present time step and the second one is linear and related to the state of the system at the next time step.

3.4. *OD2, WVV, LS and EY methods: a comparison*

We first compare the four schemes introduced in Section 3.3, looking for coherence among the different evolutions and in the values attained. In particular, we want to check that the solutions obtained evolves in the same way reaching a stable configuration.

In the provided test, the time step of each method is adjusted in order to have stable numerical solutions, in particular for OD2 $\Delta t = 5 \cdot 10^{-3}$, for LS $\Delta t = 10^{-4}$ and for EY $\Delta t = 10^{-4}$. The setting used for the simulations is the following: $\Omega = (0,1) \times (0,1)$, $u_0 = \sin(xy)$, $\tau_u = 1$, $v_0 = \cos(10(x-y))xy$, $\tau_v = 1$, $\sigma = 0.3$, $\overline{v} = \int_\Omega v_0 \approx 0.0114559$, $\epsilon_u = 0.05$, $\epsilon_v = 0.05$, $\alpha = 0.5$, $\beta = 0.8$, $T = 10$. The value of the parameters has been chosen with the same scale as the ones in [9], and the initial conditions are smooth functions with range $[-1, 1]$, which are coherent with the physical phenomenon described by the model. In all the following simulations the chosen FEM space is P_1 on a 20×20 conforming triangular mesh $\mathcal{T}_h$. In Figure 1 the snapshots of the initial conditions are reported.

As we can see in Table 1, the evolutions of u and v are very similar, both in shape and in the numerical values attained, at least for OD2, LS, and EY. In particular, we conclude that

1. OD2 method gives encouraging results: the numerical solutions seem to be physically relevant, even with "large" time steps (order 10^{-2}). We analyze in further details the output of this method in the forthcoming section;
2. Method WVV does not give reasonable outputs: even with time steps of 10^{-6} and high number of nodes, the numerical solutions tend immediately to reach very high values (order 10^6) and to oscillate very fast. Thus, we are not able to exploit this linearization method in the coupled case;
3. Methods LS and EY give accurate results only for sufficiently small time steps (order 10^{-4}).

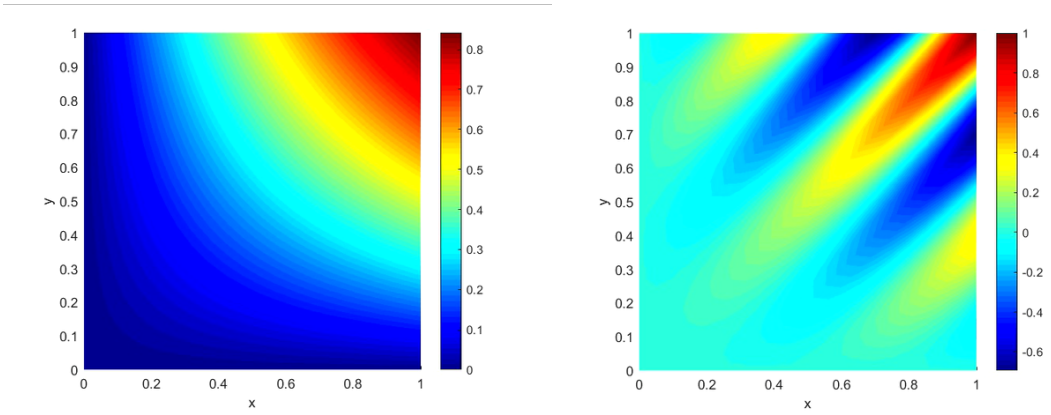

Figure 1. Initial conditions of u (left) and v (right).

The aim of the next section is to present some tests on the parameters. We perform all of them with the OD2 scheme, since it provides very similar results to the other methods and it seems to be stable with coarser time steps speeding up the computation time.

4. Fully coupled system

In this section, we verify that the numerical solutions we obtained by varying the parameters respect the physical properties of the system. To this aim, we present some tests, performed with OD2 linearization method.

Table 1. Comparison of the evolution of u and v.

Method	$t = 0.2$	$t = 2$	$t = 10$
OD2	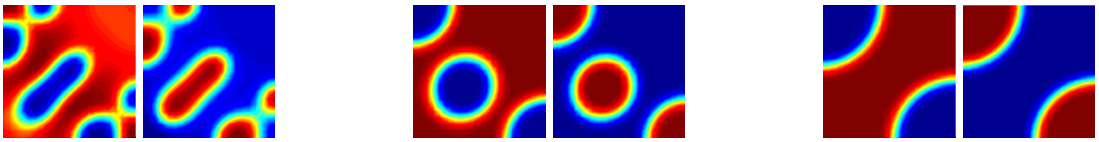		
LS	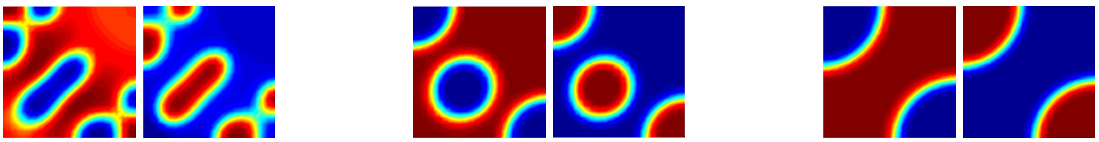		
EY	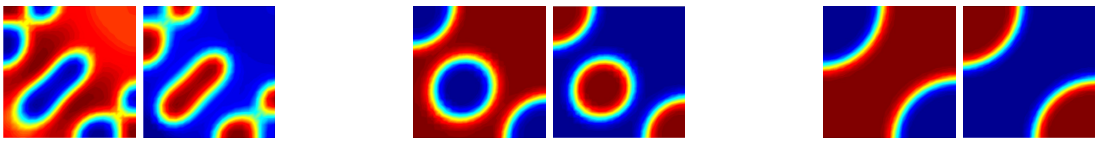		

For each test the general setting is the following: $\Omega = (0,1) \times (0,1)$, $u_0 = \sin(10xy)$, $v_0 = \cos(10(x - y))xy$, $\overline{v} = \int_\Omega v_0 \approx 0.0114559$, $\Delta t = 0.005$, $T = 15$ and the used FEM space is P_1 on a 20×20 conforming triangular mesh. For each parameter we report in a table the behavior of the solution at different times and for different values of the parameter. As initial condition for all our tests we chose smooth functions with range $[-1, 1]$, reported in Figure 2. The different values we chose for our test are inspired by [12], but not strictly related to any real experiment. In particular, we vary them in the ranges considered by the authors, in order to show the capability of the schemes to deal with parameters with the same scale of a real experiment.

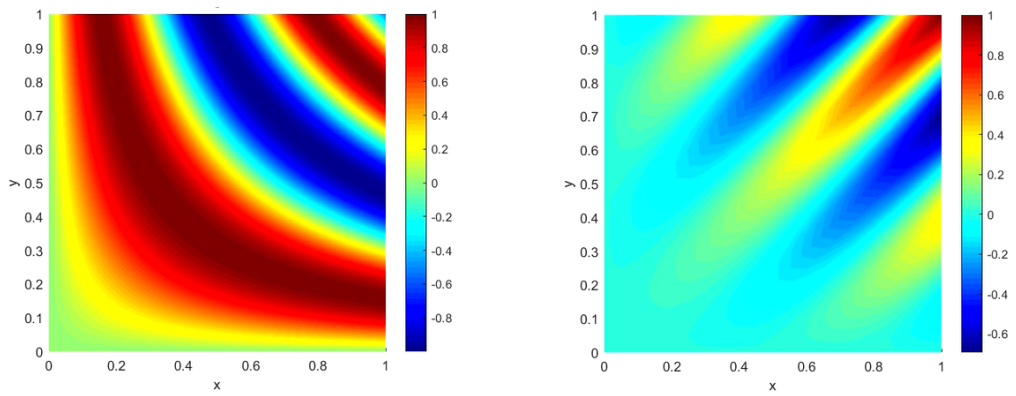

Figure 2. Initial conditions of u (left) and v (right).

4.1. *Test on* τ_v

In this test we vary the value of τ_v, in order to verify that its growth implies a slower evolution of the copolymer part of the system. As we can see in Table 2 the system reaches the same final configuration for both values of the parameter. However, for $\tau_v = 250$ it evolves slower: for $\tau_v = 10$ the part of the

copolymer in the upper-right corner has already disappered at time $t = 3$, while for $\tau_v = 250$, it is still present at time t = 6. The same happens for τ_u.

Table 2. Evolution of u (left) and v (right) with parameters $\epsilon_u = \epsilon_v = 0.05$, $\tau_u = 1$, $\sigma = 100$, $\alpha = 0.04$ and $\beta = -0.9$.

τ_v	$t = 3$	$t = 6$	$t = 15$
10	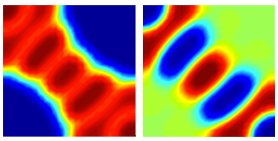	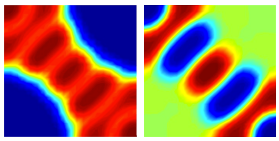	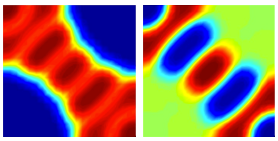
250	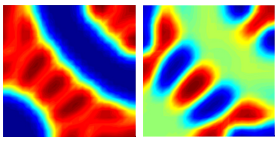	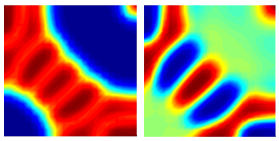	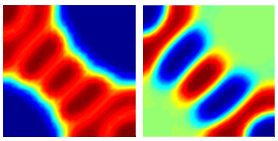

4.2. *Test on* ϵ_v

This parameter controls the separation interface thickness between the two components of the copolymer. For large values of ϵ_v the interface between the two copolymers must be thicker so that it prevents the generation of fine patterns. As we can see in Table 3, for small values of ϵ_v, we have more complicated patterns which become coarser, according to the growth of ϵ_v. The same happens for ϵ_u.

Table 3. Evolution of u (left) and v (right) with parameters $\epsilon_u = 0.05$, $\tau_u = 1$, $\tau_v = 100$, $\sigma = 60$, $\alpha = 0.02$ and $\beta = -0.9$.

ϵ_v	$t = 0.9$	$t = 6$	$t = 15$
0.03	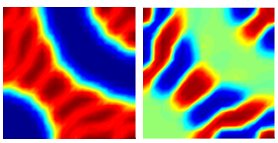	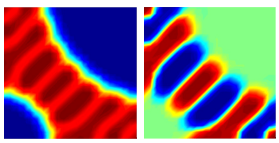	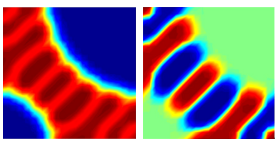
0.05	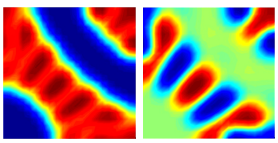	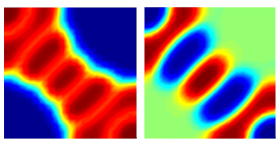	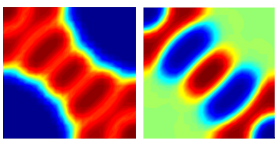

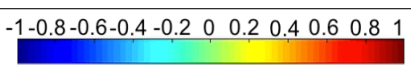

4.3. *Test on σ*

The parameter σ is related to the connectivity between the two components of the copolymer. As we can see in Table 4, as the value of σ increases, the components of the copolymer tend to separate in many small parts and do not form big macroareas.

Table 4. Evolution of u (left) and v (right) with parameters $\epsilon_u = \epsilon_v = 0.05$, $\tau_u = 1$, $\tau_v = 100$, $\alpha = 0.4$ and $\beta = -0.9$.

σ	$t = 3$	$t = 6$	$t = 15$
0	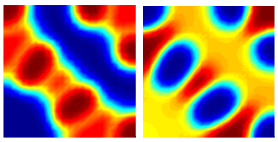	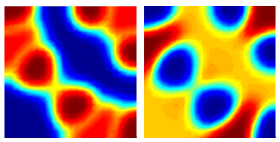	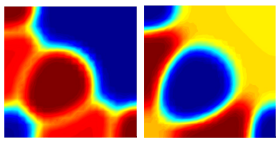
50	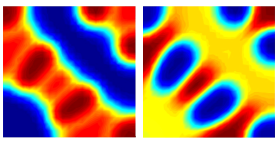	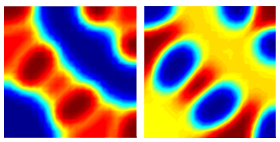	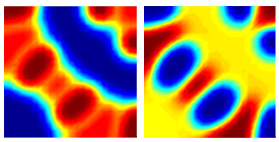
150	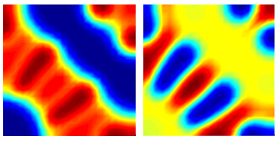	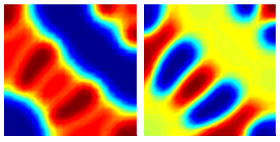	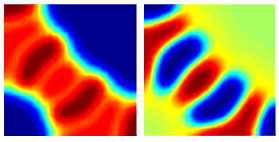
			

4.4. *Test on β*

This parameter controls the energetic interaction between u and v. As we can see in Table 5, if β decreases there is a more neat separation of the two macrophases.

Table 5. Evolution of u (left) and v (right) with parameters $\epsilon_u = \epsilon_v = 0.05$, $\tau_u = 1$, $\tau_v = 100$, $\sigma = 100$, and $\alpha = 0.01$.

β	$t = 3$	$t = 6$	$t = 15$
-0.3	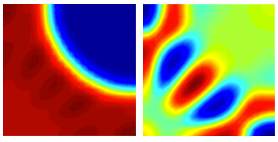	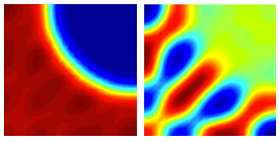	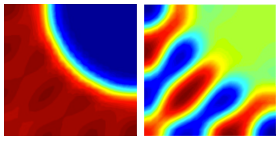
-0.5	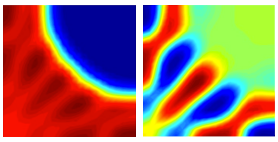	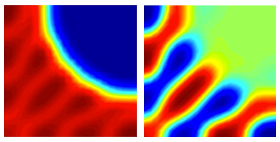	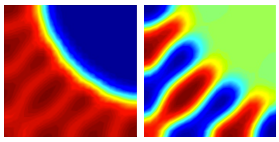
-0.9	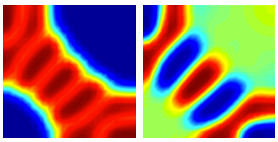	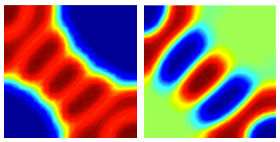	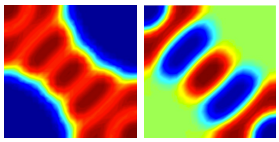
	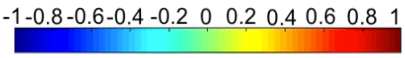		

4.5. *Test on α*

This value controls the interaction between the confined copolymer and the confining surface, causing symmetry-breaking between microphase separated domains. If $\alpha = 0$, both microphases in v can reach u with the same probability, but if $\alpha \neq 0$ we are changing the preference of u for the positive or negative values of v and thus the confining surface will change according to this preference. Indeed, as we can see in Table 6, for negative values of α, at the interface with u we have prevalence of $v = -1$, instead, with α positive, at the interface with u we have prevalence of $v = 1$.

Table 6. Evolution of u (left) and v (right) with parameters $\epsilon_u = \epsilon_v = 0.05$, $\tau_u = 1$, $\tau_v = 100$, $\sigma = 100$, and $\beta = -0.3$.

α	$t = 3$	$t = 6$	$t = 15$
-0.4	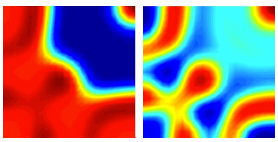	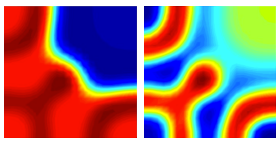	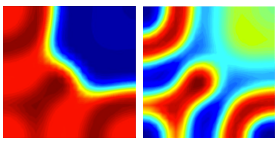
-0.08	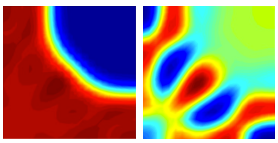	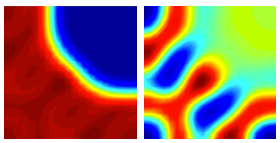	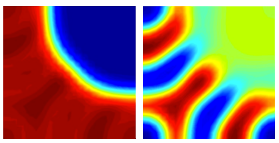
0.01	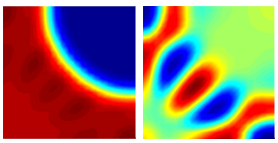	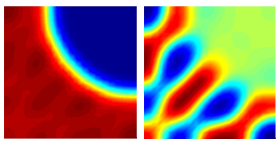	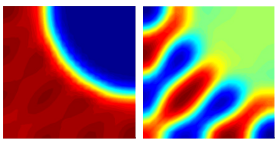
0.1	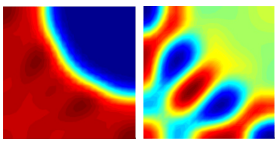	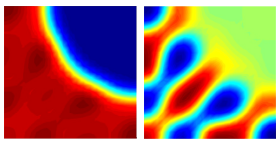	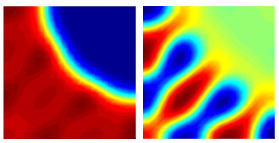
0.4	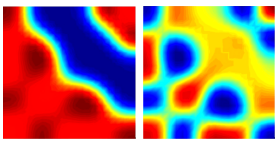	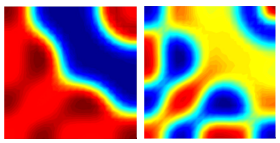	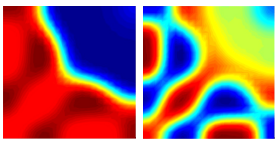

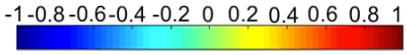

4.6. *Mass conservation*

Finally, we verify that if $\overline{v} = \int_\Omega v_0$, the quantity $\int_\Omega v(t)$ remains constant during the evolution. On the contrary, if we set an arbitrary value of $\overline{v}$ we can see that there is no mass conservation but $\int_\Omega v(t) \to \overline{v}$ as $t \to +\infty$. We report the following test in Table 7 with setting: $\Omega = (0,1) \times (0,1)$, $u_0 = \sin(10xy)$, $v_0 = \cos(10(x-y))xy$, $\Delta t = 0.005$, $T = 15$ and the FEM space we use is still P_1 on a 20×20 conforming triangular mesh.

Table 7. Evolution of v with parameters $\epsilon_u = \epsilon_v = 0.05$, $\tau_u = 1$, $\tau_v = 100$, $\sigma = 100$, and $\alpha = 0.01$, $\beta = -0.9$. Notice that $\int_\Omega v(t) = 0.01146$.

$\overline{v}$	$t = 1$	$t = 7.5$	$t = 15$
0	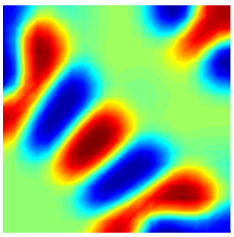 $\int_\Omega v(t) = 0.0042$	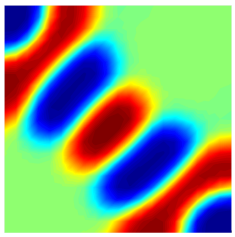 $\int_\Omega v(t) \approx 10^{-6}$	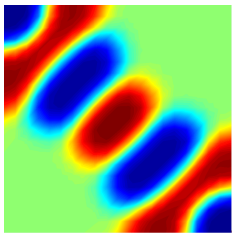 $\int_\Omega v(t) \approx 10^{-7}$
$\int_\Omega v_0$	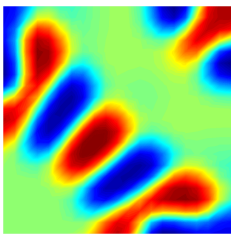 $\int_\Omega v(t) = 0.01139$	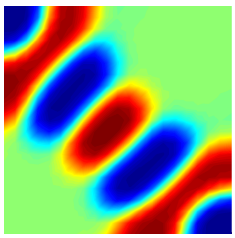 $\int_\Omega v(t) = 0.01146$	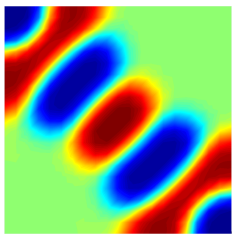 $\int_\Omega v(t) = 0.01146$
0.6	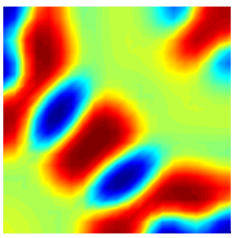 $\int_\Omega v(t) = 0.38179$	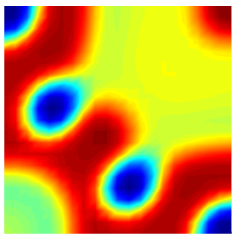 $\int_\Omega v(t) = 0.59967$	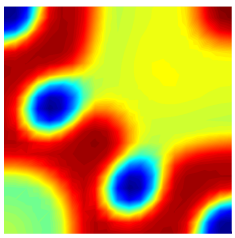 $\int_\Omega v(t) = 0.59999$

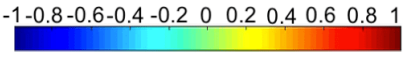

5. Conclusions

We have proposed and tested different strategies to provide a numerical approximation of the solution of a system of fully coupled Cahn-Hilliard equations. The numerical solutions we have obtained seem to give a fair description of the physical process, for example we can see that the evolution of the copolymer is confined where $u = 1$. We highlight that the solution behaves coherently with the phenomenon without imposing conditions at the interface.

Our results in the two-dimensional framework are in accordance with the ones in [9], even if we consider Neumann boundary conditions instead of periodic. From a numerical point of view, we notice that at least two of the linearization methods used for the single Cahn-Hilliard equation (OD2 and EY) may be used also in the context of the coupled system. Moreover, the results are good even with a coarse grid in space (20×20) and with a low order (i.e 1) FEM approximations.

This work represents a first step in developing efficient numerical methods for fully coupled systems of Cahn-Hilliard equations: even if we do not provide a theoretical analysis of our schemes, our results are encouraging. Then, it may be interesting to further carry out some experimental validations and to fully address the theoretical part. From an analytical point of view, the study of the well posedness, regularity and longtime behavior of the solutions is also a topic of further research.

Acknowledgements

We gratefully thank Prof. P. F. Antonietti and Prof. M. Grasselli for suggesting the problem and for many helpful discussions.

References

1. J. Cahn, On spinodal decomposition, *Acta Metallurgica*, vol. 9, pp. 795–801, 1961.
2. J. E. Hilliard and J. W. Cahn, Free energy of a non-uniform system. iii. nucleation in a two-component incompressible fluid, *The Journal of Chemical Physics*, vol. 31, pp. 688–699, 1959.
3. J. E. Hilliard and J. W. Cahn, Free energy of a non-uniform system. i. interfacial free energy, *The Journal of Chemical Physics*, vol. 28, pp. 258–267, 1958.
4. L. Q.-X., D. A., V. Rottschafer, M. de Jager, P. M. J. Herman, R. M., and J. Van de Koppel, Phase separation explains a new class of self-organized spatial patterns in ecological systems, *Proceedings of the National Academy of Sciences of the USA*, vol. 110, pp. 11905–11910, 2013.
5. S. Tremaine, On the origin of irregular structure in saturn's rings, *The Astronomical Journal*, vol. 125, pp. 894–901, 2003.
6. S. M. Wise, J. S. Lowengrub, H. B. Frieboes, and V. Cristini, Three-dimensional multispecies nonlinear tumor growth-i: Model and numerical method, *Journal of Theoretical Biology*, vol. 253, pp. 524–543, 2008.
7. J. Huh, D. Jeong, J. Kim, D. Lee, J. Shin, and A. Yun, Physical, mathematical, and numerical derivations of the cahn-hilliard equation, *Computational Materials Science*, vol. 81, pp. 216–225, 2014.
8. A. Miranville, The cahn-hilliard equation and some of its variants, *AIMS Mathematics*, vol. 2, pp. 479–544, 2017.
9. E. Avalos, T. Higuchi, T. Teramoto, H. Yabu, and Y. Nishiura, Frustrated phases under three-dimensional confinement simulated by a set of coupled cahn-hilliard equations, *Soft Matter*, vol. 12, pp. 5905–5914, 2016.
10. D. Eyre, An unconditionally stable one-step scheme for gradient systems. unpublished article, 1998.
11. T. Teramoto and Y. Nishiura, Morphological characterization of the diblock copolymer problem with topological computation, *Japan Journal of Industrial and Applied Mathematics*, vol. 27, pp. 175–190, 2010.
12. E. Avalos, T. Higuchi, T. Teramoto, H. Yabu, and Y. Nishiura, Electronic supplementary information for soft matter manuscript: Frustrated phases under three-dimensional confinement simulated by a set of coupled cahn-hilliard equations.
13. T. Ohta and K. Kawasaki, Equilibrium morphology of block copolymer melts, *Macromolecules*, vol. 19, pp. 2621–2632, 1986.
14. A. Quarteroni, *Numerical models for differential problems*. Springer International Publishing, 2017.
15. F. Guillen-Gonzales and G. Tierra, On linear schemes for a cahn-hilliard diffuse interface model, *Journal of Computational Physics*, vol. 234, pp. 140–171, 2013.
16. X. Wu, G. Van Zwieten, and K. Van der Zee, Stabilized second-order convex splitting schemes for cahn-hilliard models with application to diffuse-interface tumor-growth models, *International Journal for Numerical Methods in Biomedical Engineering.*, vol. 30, pp. 180–203, 2014.
17. D. Eyre, Unconditionally gradient stable time marching the cahn-hilliard equation, *MRS Proceedings*, vol. 529, 1998.